JCTC Journal of Chemical Theory and Computation

Algorithm for Generating Defective Graphene Sheets

David R. Nutt*,† and Hilary Weller‡

Department of Chemistry, University of Reading, PO Box 224, Whiteknights, Reading, RG6 6AD, U.K., and National Centre for Atmospheric Science—Climate, Department of Meteorology, University of Reading, PO Box 243, Earley Gate, Reading, RG6 6BB, U.K.

Received March 10, 2009

Abstract: An algorithm is presented for the generation of molecular models of defective graphene fragments, containing a majority of 6-membered rings with a small number of 5- and 7-membered rings as defects. The structures are generated from an initial random array of points in 2D space, which are then subject to Delaunay triangulation. The dual of the triangulation forms a Voronoi tessellation of polygons with a range of ring sizes. An iterative cycle of refinement, involving deletion and addition of points followed by further triangulation, is performed until the user-defined criteria for the number of defects are met. The array of points and connectivities are then converted to a molecular structure and subject to geometry optimization using a standard molecular modeling package to generate final atomic coordinates. On the basis of molecular mechanics with minimization, this automated method can generate structures, which conform to user-supplied criteria and avoid the potential bias associated with the manual building of structures. One application of the algorithm is the generation of structures for the evaluation of the reactivity of different defect sites. Ab initio electronic structure calculations on a representative structure indicate preferential fluorination close to 5-ring defects.

Introduction

There is currently a growing interest in carbon structures based on 5-, 6-, and 7-membered rings.[1] The archetypal example is C_{60}, in which twelve pentagonal rings are distributed among twenty hexagonal rings in a football-like structure, such that no pentagon is adjacent to another pentagon.[2] The subsequent discovery of carbon nanotubes,[3] nanohorns,[4] and the associated nanoparticle side-products[5] provide a wide-range of contrasting structures and topologies, all of which are likely to contain a certain number of defects.[6]

It is well-known that nonhexagonal rings introduce curvature into an otherwise-planar graphitic sheet.[7] Introduction of an n-gon into a fragment of a graphene, where $n < 5$, leads to the formation of cones. When $n = 5$, fullerene-type structures emerge, and for $n > 6$, the negative curvature leads to saddle-like surfaces. As n is increased further (up to $n = 24$), calculations predict complex but stable distorted structures.[8]

Because of the stability of nonhexagonal rings in carbon structures, a number of groups have started to investigate whether there is evidence for polygonal defects in a number of carbon forms including nongraphitising (microporous) carbon,[9] glassy carbon,[10,11] and carbon black.[12] In many cases, it appears that incorporation of polygonal defects can help explain some of their many characteristics, such as low density, microporosity, and hardness.[1] Recent transmission electron microscopy (TEM) studies have demonstrated exceptional resolution, confirming the presence of 5-membered rings in samples of activated carbon[13] and providing atomic-level insight into the edges of graphene layers.[14]

Theoretical investigation of such structures can also yield useful insight. These can involve calculations of energy pathways involved in reconstructions, such as the Stone—Wales rearrangement in C_{60}[15] or the reconstruction of graphene edges.[16] Calculation of experimental observables, such as scanning tunnelling microscopy (STM) images, provides a

* To whom correspondence should be addressed. Telephone: +44-118-3786346. Fax: +44-118-3786331. E-mail: d.nutt@reading.ac.uk.

† Department of Chemistry.

‡ National Centre for Atmospheric Science—Climate.

10.1021/ct900113f CCC: $40.75
Published on Web 06/23/2009

direct comparison between experiment and theory and helps in the interpretation of experimental data.[17] Semiempirical or ab initio electronic structure calculations can provide information about reactive sites available for functionalization[18] or vibrational modes.[19]

However, the first stage of any theoretical investigation is the generation of a suitable structure. For small systems with a single defect, this is straightforward. It is possible to construct one *n*-gonal defect in a graphene sheet by joining *n* 60° segments of graphene together at a point.[8,17] Many such structures can be made "by hand", although this removes any randomness from the resulting structure and may lead to bias in the features created. For this reason, it is good to be able to automate the generation of suitable structures. Since the systematic determination of structures rapidly becomes a very large task,[20] molecular dynamics (MD)[21] or reverse Monte Carlo (RMC) methods are often used.[9] Experimentally, the growth of graphene on metal surfaces appears to occur by the addition of carbon cluster attachment.[22] Modeling of this process would offer an alternative method for generating graphene structures.

In this paper, a novel algorithm is presented for the automated generation of small graphene fragments containing small numbers of 5- and 7-ring defects. This algorithm is based on a Delaunay triangulation of a 2D array of points, followed by subsequent refinement. This new algorithm allows the user to define acceptable ratios of ring-sizes, based on experimental data, for example, but is otherwise designed around an initial random distribution of points, removing the potential for bias. Once a structure has been generated, energy minimization using classical molecular mechanics generates atomic coordinates, which can then be used in ab initio electronic structure calculations to identify sites for functionalization via fluorination[23,24] or electrochemical methods.[25]

Since the details and rationalization of the fluorination products of fullerenes and carbon nanotubes are still under debate,[23,24,26,27] the energetics of fluorination at isolated defects, such as those present in the graphene structures generated in the present work, can provide useful insight into the preferred regiochemistry.

Methods

Generation of an Initial Network. An initial distribution of points in 2-dimensional space was produced using a Sobol quasirandom sequence.[28,29] Quasirandom sequences have the property that they cover space "more uniformly" than true random sequences. As a result, they are often used in the numerical evaluation of high-dimensional integrals and global optimisation problems. Triangulation of these points, inserting additional Steiner points to avoid formation of triangles with internal angles smaller than 20°, was performed using the program Triangle.[30] The dual of the triangulation produces a Voronoi tessellation with a distribution of ring sizes. This process is illustrated in Figure 1.

The remaining task is therefore the conversion of the Voronoi tessellation from an abstract network of points to a structure with a connectivity typical of a molecular system,

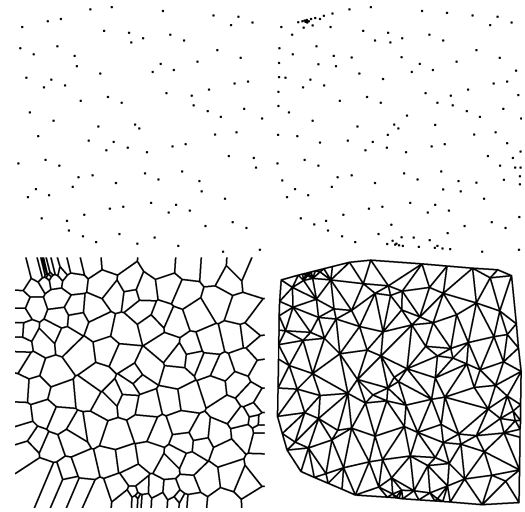

Figure 1. Processes during the generation of graphene-type networks. Clockwise from top-left: initial random points, initial points with additional Steiner points to increase the quality of the triangulation, Delaunay triangulation of the points, corresponding Voronoi tessellation.

in which the vertices are atoms and the edges represent chemical bonds. In the case of interest here, graphene, chemical knowledge dictates that the Voronoi tessellation must fulfill the following rules (Voronoi Rules):

(1) The network is limited to 5, 6, and 7-membered rings, with ratios as determined from experiments.
(2) Vertices must have a maximum connectivity of three (the connectivity is lower at the edges of a finite sheet).

The dual relationship between the Voronoi tessellation and the Delaunay triangulation leads to the following rule for the triangulation (Triangulation Rule):

(1) Vertices must have a connectivity of 5, 6, or 7, unless the point lies on the boundary, in which case the connectivity may be smaller.

Voronoi and Triangulation Rule 1 can be addressed by deleting or adding points to the triangulation in a well-defined way until the network complies (described below). Voronoi Rule 2 does not require an additional Triangulation Rule, since the triangulation is conforming Delaunay, meaning that all Voronoi vertices will automatically have a connectivity of three (except at the edge of the tessellation).

Modifying the Network to Comply with Chemical Knowledge. In the following, the connectivity in the triangulation is represented by c. Any point with $c < 5$ and not on the boundary of the triangulation was removed from the network. All points (x,y) with $c > 7$ were divided into two points (x_1,y_1) and (x_2,y_2), where $q_1 = q + \varepsilon_q$ and $q_2 = q - \varepsilon_q$, where q represents x or y and ε_q is a random number, small with respect to the interpoint distances.

All points with $c = 6$ were retained. Points with $c = 5,7$ were deleted or divided, respectively, according to a Monte Carlo procedure, with the acceptance and rejection probabilities chosen as free parameters. A number of additional points were also added to the convex hull of the triangulation, also in a Monte Carlo-type procedure, in order to reduce the number of unphysically long edges. The number of 5-, 6-, and 7-membered rings was determined and the current

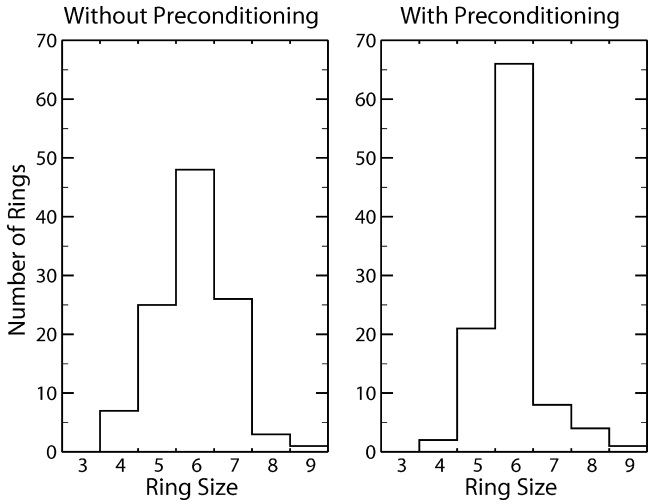

Figure 2. Distribution of ring sizes for a set of points without (left) and with (right) preconditioning.

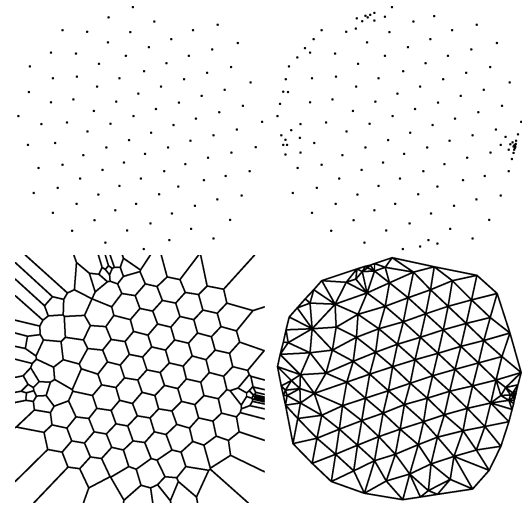

Figure 3. Processes during the generation of graphene sheets, with preconditioning. Clockwise from top-left: initial random points following relaxation, initial points with additional Steiner points to increase the quality of the triangulation, Delaunay triangulation of the points, corresponding Voronoi tessellation.

pentagon/hexagon and heptagon/hexagon ratios calculated. These are then compared with the target ratios determined from chemical knowledge of graphene systems, typically pentagon/hexagon = 3/100 and heptagon/hexagon = 1/100,[31] and compliance with the Triangulation Rule is checked. If all target ratios and network criteria are fulfilled, the network is accepted. Otherwise, further cycles of triangulation are performed (with no further addition of Steiner points) until convergence is found.

Geometry Optimization. Once a satisfactory network of points has been created, this can be converted into a chemical structure with atoms and bonds. In the present work, the structure was imported into the Charmm program,[32] each atom was assigned parameters corresponding to an aromatic carbon atom in the Charmm22 parameter set,[33] and the structure was minimized using Steepest Descent or Newton−Raphson methods to a gradient tolerance of 1×10^{-7} kcal/mol/Å.

Preconditioning of the Triangulation Points. Convergence of the above algorithm is typically slow. This is because no relaxation of the triangulation points is allowed during the refinement, leading to a broad distribution of connectivities and therefore a broad range of ring sizes in the Voronoi tessellation. Refinement is therefore slower, since a larger number of unsuitable rings must be eliminated before convergence is reached. This can be alleviated by allowing relaxation.

A close-packed network of points in a plane produces a perfect triangular network, the dual of which is a network of hexagons. Relaxation of points in a plane will move toward close-packing, giving a narrower distribution of connectivities in the network with a sharp peak at a connectivity of 6, as shown in Figure 2.

Each cycle of refinement (adding/deleting points) was therefore followed by relaxation. Each point was modeled as a lone aromatic carbon atom with the same parameters as above, and energy minimization was performed using the steepest descent algorithm in the Charmm program. Only a small number of minimization steps were performed, to remove as many unsuitable connectivities as possible through local rearrangements, while retaining a certain number of 5- and 7-connective defects, as required. Further minimization effectively leads to the removal of defects from the interior of the lattice through annealing. For comparison with the initial process (Figure 1), a corresponding set of figures showing the process with preconditioning is shown in Figure 3. It is clear that the topology of the final Voronoi tessellation is much closer to that of graphene.

Electronic Structure Calculations. Ab initio electronic structure calculations were performed on a small, defective graphene sheet to determine the most favorable sites for functionalization of the graphene sheet by fluorination. Hydrogen atoms were added around the edge of the sheet to satisfy bonding and ensure a closed-shell singlet ground state. Full geometry optimizations were performed for all fluorination sites on the mainly convex side of the sheet (an additional hydrogen atom was added to the periphery of the sheet to maintain the singlet electronic state), using the Gamess-UK electronic structure program[34] at the HF/3-21G* level. The energies of the optimized structures were then compared to determine the thermodynamically most-favorable fluorination site. Because many finite graphene-type structures have been shown to possess a spin-polarized ground state, even with a perfect hexagonal lattice and edge passivation,[35−38] tests were carried out to ensure that the ground state of the molecular system was neither magnetic nor metallic. Geometry optimizations using both spin-restricted and unrestricted Hartee Fock formalisms were performed for the original graphene structure and for the lowest energy fluorinated structure. In each case, the calculations yielded identical structures and energies. Visual inspection of the frontier molecular orbitals (HOMO−1, HOMO, LUMO, LUMO+1) revealed no differences for α and β electrons in the UHF calcula-

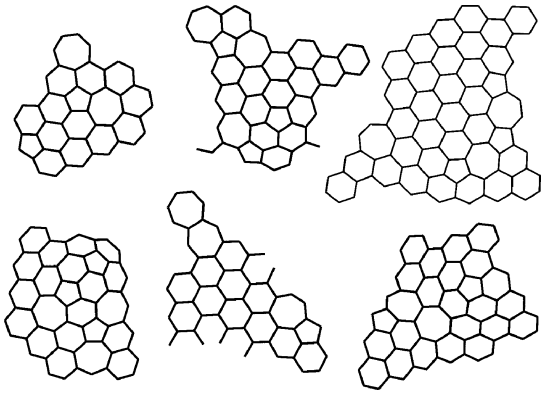

Figure 4. A selection of small defective graphene sheets generated using the new algorithm.

tions. As a result, the spin-restricted Hartree−Fock method was deemed to be appropriate.

Results

Small Structures. For a target ratio of ring sizes (pentagon/hexagon, heptagon/hexagon) of 0.2−0.3, small systems can be generated, with tens of rings. These can be generated with no preconditioning, starting from initial arrays of ∼100 points. A selection of energy-minimized structures are shown in Figure 4. Such structures are suitable for use in ab initio electronic structure calculations to probe the reactivity at various sites relevant to functionalization (see below).

Larger Structures. For smaller target ratios, such as pentagon/hexagon = 0.03 and heptagon/hexagon = 0.01, larger systems with hundreds of rings must be constructed for defects to be observed. This creates certain difficulties in automated production of suitable networks. One particular feature of the Voronoi tessellations produced by the above algorithm is that the majority of pentagonal defects are found around the edges of the network, especially at the armchair edges. This can be observed in Figures 1 and 3. This is an artifact of the calculation of Voronoi tessellation for finite systems. If these edges are included in the final network, not only will the number of pentagonal rings be much higher than required by the target ratio, but the system is also not likely to be representative of extended graphene sheets. However, they are likely to be of relevance for edge effects in graphene, where reconstructions are found to occur.[16]

To avoid introduction of these artifacts, structures were cut from the central region of a tessellation. As the relaxation of the sheet and growth around the edges (because of the addition of extra vertices along long edges) was found to occur in an isotropic manner (the circular nature of the relaxed network is obvious in Figure 3), a circle with a radius of approximately half the maximum radius was cut from the large network. Although it is possible to cut other geometric or random shapes from an extended sheet with no changes to the algorithm, we restrict ourselves to circles for simplicity.

Two representative structures obtained with target ratios of 0.03 (pentagon/hexagon) and 0.01 (heptagon/hexagon) are shown in Figure 5.

The structures generated by the algorithm are governed by a number of parameters, including the probability of dividing and deleting a vertex. Increasing these probabilities leads to an increase or reduction in the number of atoms in the final structure, respectively, as illustrated in Figure 6. The parameters used in the current work are provided in Table 1.

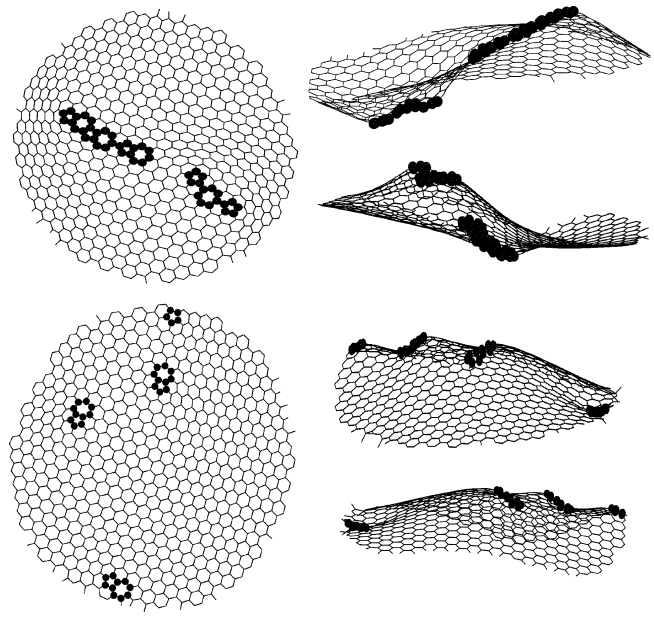

Figure 5. Two defective graphene sheets generated using the new algorithm. Side views of the sheet (revealing curvature) are placed adjacent to the planar view. Atoms forming defect rings are shown in a ball and stick representation.

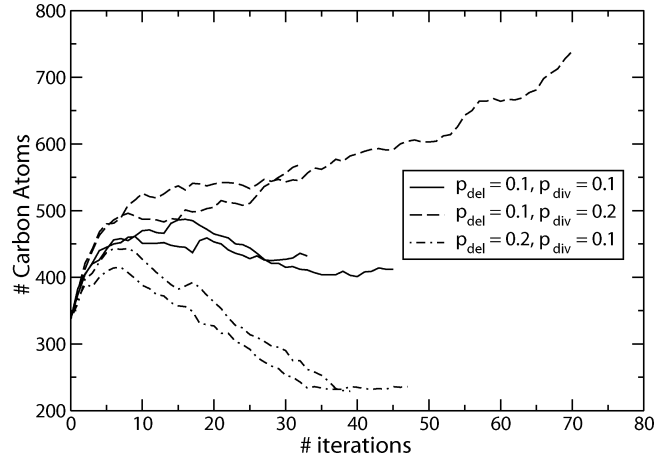

Figure 6. Effect of the probability for the deletion/division of points on the total number of carbon atoms in the structures created for six individual calculations, all of which converged to a valid structure.

Table 1. Free Parameters Used in the Refinement of a 625-Vertex Data Set

probability of deleting a vertex	0.1
probability of dividing a vertex	0.1
probability of adding a vertex to a boundary edge	0.5
min. length of a boundary edge before creation of a midpoint (Å)	10
initial number of minimization steps	500
subsequent number of minimization steps	50

Distribution of Rings. In the structures illustrated in Figure 5, it is noteworthy that 5-ring and 7-ring defects tend

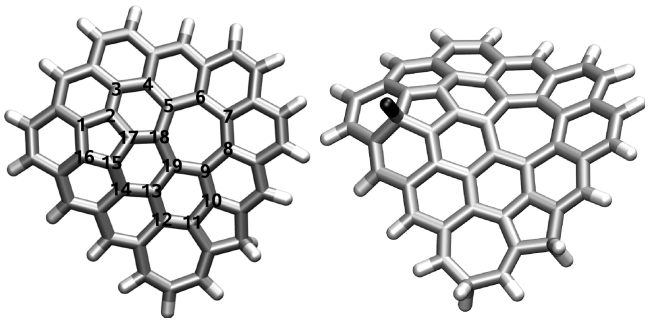

Figure 7. Left: The initial graphene structure showing the numbering of possible fluorination sites. Right: Structure of the most stable fluorinated structure.

to be found close to each other. This is due, in part, to the preconditioning process, in which defects are annealed out to obtain the required defect ratios, resulting in regions of perfect hexagonal ordering with isolated groups of defects. This could be avoided by introducing a more complex preconditioning process, involving a full three-dimensional treatment of the mesh. However, additional experimental data on the proximity of 5- and 7-ring defects would be required before the inclusion of further complexity can be justified.

Identifying the Most Favorable Sites for Fluorination Using Electronic Structure Calculations. The preferred sites for fluorination of a representative graphene structure were determined by ab initio electronic structure calculations. The initial structure contained 2 seven-membered rings, 2 five-membered rings, and 12 six-membered rings, with a total of 47 carbon atoms and is shown in Figure 7. Eighteen hydrogen atoms were added around the edge of the sheet to satisfy bonding and ensure a closed-shell singlet ground state. The relative energies and the local topology of the 19 fluorination isomers investigated are shown in Table 2, with the numbering of the fluorination sites and the lowest energy structure as illustrated in Figure 7. HOMO−LUMO gaps varied between 2 and 6 eV, indicating that the structures are not metallic. It can be seen that most of the low-energy structures are those in which the fluorination occurs at or close to the internal 5-membered ring. This can be rationalized by the positive curvature which already exists at a 5-ring defect. Only a small distortion of the carbon framework is then required to add an additional bonded neighbor and form a tetrahedral carbon atom. Many of the high-energy sites are those around the internal 7-membered ring, where the negative curvature makes it unfavorable to add a fourth bonded neighbor. However, the details are not so clear-cut. Significant distortions of the 7-membered ring appear to be tolerated at some positions making fluorination at sites 18 and 19 more favorable than would perhaps be expected. It is likely that this is caused by the proximity of the 5-membered ring

Table 2. Relative Energies of a Fluorinated Graphene Sheet with Defects

site	E_{rel}/kJ mol^{-1}	local topology[a]
16	0.0	5−6−6
2	87.9	5−6−6
14	114.1	6−6−6
18	154.3	6−6−7
19	196.4	6−6−7
17	200.2	5−6−6
10	213.2	5−6−6
15	216.4	5−6−6
6	232.4	6−6−7
12	234.3	6−6−7
1	238.7	5−5−6
11	249.2	5−6−7
13	267.7	6−6−6
8	269.1	6−6−7
4	282.8	6−6−6
3	287.9	6−6−6
9	309.9	6−6−7
5	319.0	6−6−7
7	333.6	6−6−7

[a] The local topology is defined in terms of the sizes of the three rings that share a common vertex at the position in question. For example, a vertex that is shared between three 6-membered rings (and hence expected to be in a locally planar environment) is labeled "6−6−6". The local topology gives an indication of the expected curvature (zero, positive, negative) of the graphene fragment at the position of interest.

Conclusions

A rapid and robust algorithm has been developed to facilitate the automated generation of graphene sheets containing a majority of 6-membered rings, with a small, user-specified, number of 5- and 7-ring defects.

In comparison with existing methods,[9,21] this algorithm allows the generation of small fragments of graphene (tens to thousands of atoms) according to user-defined criteria within a few minutes on a desktop PC. There is no requirement for periodic boundary conditions or computationally expensive simulations (which can be of the order of days[9]). After initial generation of set of random coordinates, which in the present work requires no special procedures to fulfill artificial periodicity or chemical bonding requirements, the central iterative procedure uses deterministic methodology (triangulation followed by minimization). Chemical information, in the form of an interatomic potential, is only added for the minimization step (which represents the most expensive part of the procedure). Chemical bonding is determined solely by the results of triangulation (which also automatically ensures the correction coordination number), meaning that no special procedures need to be incorporated in order to control bond making and breaking processes.[9,21] As a result, the algorithm presented here provides a simple and efficient solution to the generation of small, defective graphene sheets.

Once generated, these structures can be used in electronic structure calculations to identify favorable sites for functionalization by fluorination. The results obtained indicate that fluorination will occur preferentially at 5-ring defects, although the overall energetics depend on the details of the local topology. A further use of the structures generated could be in the simulation of STM images, providing a further tool for the interpretation and understanding of experimental observations.

Acknowledgment. D.R.N. is grateful to Peter Harris for introducing him to this interesting problem and for helpful discussions.

References

(1) Harris, P. J. F. *Crit. Rev. Solid State Mater. Sci.* **2005**, *30*, 235–253.

(2) Kroto, H. W.; Heath, J. R.; O'Brien, S. C.; Curl, R. F.; Smalley, R. E. *Nature* **1985**, *318*, 162–163.

(3) Iijima, S. *Nature* **1991**, *354*, 56–58.

(4) Iijima, S.; Yudasaka, M.; Yamada, R.; Bandow, S.; Suenaga, K.; Kokai, F.; Takahashi, K. *Chem. Phys. Lett.* **1999**, *309*, 165–170.

(5) Bandow, S.; Kokai, F.; Takahashi, K.; Yudasaka, M.; Qin, L. C.; Iijima, S. *Chem. Phys. Lett.* **2000**, *321*, 514–519.

(6) Charlier, J. C. *Acc. Chem. Res.* **2002**, *35*, 1063–1069.

(7) Iijima, S.; Ichihashi, T.; Ando, Y. *Nature* **1992**, *356*, 776–778.

(8) Ihara, S.; Itoh, S.; Akagi, K.; Tamura, R.; Tsukada, M. *Phys. Rev. B* **1996**, *54*, 14713–14719.

(9) Kumar, A.; Lobo, R. F.; Wagner, N. J. *Carbon* **2005**, *43*, 3099–3111.

(10) Harris, P. J. F. *Phil. Mag.* **2004**, *A84*, 3159–3167.

(11) Gogotsi, Y.; Libera, J. A.; Kalasknikov, N.; Yoshimura, M. *Science* **2000**, *290*, 317–320.

(12) Goel, A.; Hebgen, P.; Vander Sande, J. B.; Howard, J. B. *Carbon* **2002**, *40*, 177–182.

(13) Harris, P. J. F.; Liu, Z.; Suenaga, K. *J. Phys.: Condens. Matter* **2008**, *20*, 362201.

(14) Liu, Z.; Suenaga, K.; Harris, P. J. F.; Iijima, S. *Phys. Rev. Lett.* **2009**, *102*, 015501.

(15) Stone, A. J.; Wales, D. J. *Chem. Phys. Lett.* **1986**, *128*, 501–503.

(16) Koskinen, P.; Malola, S.; Häkkinen, H. *Phys. Rev. Lett.* **2008**, *101*, 115502.

(17) Kobayashi, K. *Phys. Rev. B* **2000**, *61*, 8496–8500.

(18) Ormsby, J. L.; King, B. T. *J. Org. Chem.* **2007**, *72*, 4035–4038.

(19) Malola, S.; Häkkinen, H.; Koskinen, P. *Phys. Rev. B* **2008**, *77*, 155412.

(20) Tošić, R.; Mašulović, D.; Stojmenović, I.; Brunvoll, J.; Cyvin, B. N.; Cyvin, S. J. *J. Chem. Inf. Comput. Sci.* **1995**, *35*, 181–187.

(21) Shi, Y. *J. Chem. Phys.* **2008**, *128*, 234707.

(22) Loginova, E.; Bartelt, N. C.; Feibelman, P. J.; McCarty, K. F. *New J. Phys.* **2008**, *10*, 093026.

(23) Mickelson, E. T.; Huffman, C. B.; Rinzler, A. G.; Smalley, R. E.; Hauge, R. H.; Margrave, J. L. *Chem. Phys. Lett.* **1998**, *296*, 188–194.

(24) Claves, D.; Rossignol, J. *Chem. Phys. Lett.* **2009**, *468*, 231–233.

(25) Ghanem, M. A.; Chrétien, J.-M.; Pinczewska, A.; Kilburn, J. D.; Bartlett, P. N. *J. Mater. Chem.* **2008**, *18*, 4917–4927.

(26) Selig, H.; Lifshitz, C.; Peres, T.; Fischer, J. E.; McGhie, A. R.; Romanow, W. J.; McCauley, J. P.; Smith, A. B., III *J. Am. Chem. Soc.* **1991**, *113*, 5475–5476.

(27) Jia, J. F.; Wu, H. S.; Xu, X. H.; Zhang, X. M.; Jia, H. H. *J. Am. Chem. Soc.* **2008**, *130*, 3985–3988.

(28) Sobol, I. M. *USSR Comput. Math. Math. Phys.* **1967**, *7*, 86–112.

(29) Press, W. H.; Teukolsky, S. A.; Vetterling, W. T.; Flannery, B. P. *Numerical Recipes in Fortran*, 2nd ed.; Cambridge University Press: Cambridge, UK, 1992; pp 299−305.

(30) Shewchuk, J. R. Triangle: Engineering a 2D Quality Mesh Generator and Delaunay Triangulator. In *Applied Computational Geometry: Towards Geometric Engineering*; Lin, M. C., Manocha, D. , Eds.; Springer-Verlag: Berlin, Germany, 1996; Vol. 1148, pp 203−222.

(31) Harris, P. J. F. Personal communication, 2008.

(32) Brooks, B. R.; Bruccoleri, R. E.; Olafson, B. D.; States, D. J.; Swaminathan, S.; Karplus, M. *J. Comput. Chem.* **1983**, *4*, 187–217.

(33) MacKerell, A. D., Jr. *J. Phys. Chem. B* **1998**, *102*, 3586–3616.

(34) Guest, M. F.; Bush, I. J.; van Dam, H. J. J.; Sherwood, P.; Thomas, J. M. H.; van Lenthe, J. H.; Havenith, R. W. A.; Kendrick, J. *Mol. Phys.* **2005**, *103*, 719–747.

(35) Ezawa, M. *Phys. Rev. B* **2007**, *76*, 245415.

(36) Fernández-Rossier, J.; Palacios, J. J. *Phys. Rev. Lett.* **2007**, *99*, 177204.

(37) Kudin, K. N. *ACS Nano* **2008**, *2*, 516–522.

(38) Hod, O.; Scuseria, G. E. *ACS Nano* **2008**, *2*, 2243–2249.

CT900113F